



Establishing a novel and sensitive assay for bioactivity determination of anti-CD25 antibodies

Maoqin Duan¹, Chuanfei Yu¹, Yalan Yang¹, Zhihao Fu, Chunyu Liu, Jialiang Du, Meng Li, Sha Guo, XiaoJuan Yu, Gangling Xu, Yuting Mei, Lan Wang^{*}

Key Laboratory of the Ministry of Health for Research on Quality and Standardization of Biotech, Division of Monoclonal Antibody Products, National Institutes for Food and Drug Control, Beijing 102629, China

ARTICLE INFO

Keywords:

Anti-CD25 antibody
IL-2
Reporter gene assay
Bioassay

ABSTRACT

Anti-CD25 antibodies have been approved for renal transplantation and has been used prior to and during transplantation by the Food and Drug Administration (FDA). However, no reported bioassays have been reflected the mechanism of action (MOA) of anti-CD25 antibodies. Here, we describe the development and validation of a reporter gene assay (RGA) based on the engineered C8166-STAT5RE-Luc cells expressing endogenous IL-2 receptors and a STAT5-inducible element-driven firefly luciferase in C8166 cell lines. The RGA was fully validated according to the International Conference on the Harmonization of Technical Requirements for the Registration of Pharmaceuticals for the Human Use-Q2 (ICH-Q2). After optimization, the assay showed excellent specificity, linearity, accuracy, precision, and robustness. Due to the MOA relatedness and the excellent assay performance, the RGA is suitable for exploring the critical quality attributes (CQAs), release inspection, comparability and stability of anti-CD25 mAbs.

1. Introduction

The diversity of cell types involved in homeostasis and immune responses are regulated by interleukin-2 (IL-2), which was firstly discovered in 1976 as a lymphocyte growth factor with a size of 15 kDa [1]. IL-2R α (CD25), IL-2R β (CD122), and IL-2R γ (CD132) constitute heterotrimeric receptor and its expression levels depends on immune cell activation state [2,3]. The expression of IL-2R is essential for IL-2 signal transduction and also plays a role in a variety of functions in cell differentiation, survival, and effector functions. IL-2 signals through the JAK/STAT pathway followed by a succession of signaling cascades that rely on the principal signaling molecule STAT5 [4–7].

A recombinant murine and human chimeric IgG1 kappa monoclonal antibody (mAb), Basiliximab, which targets the alpha subunit of CD25, was approved to be used in renal transplant patients as an induction agent prior to and during transplantation in the United States since 1998 [3,8]. T cells expressing the IL-2R release pro-inflammatory cytokines after binding with IL-2. Basiliximab has a strong and specific affinity for CD25 on the surface of activated T-cells to play the role of restraint T cell activation, proliferation, and response in transplant recipients [9–11]. Furthermore, Basiliximab has been shown to improve long-term graft and patient survival via

^{*} Corresponding author. Division of Monoclonal Antibody Products, National Institutes for Food and Drug Control, 31# HUATUO Road, Beijing 102629, China.

E-mail address: wanglan@nifdc.org.cn (L. Wang).

¹ These authors contributed equally to this study.

<https://doi.org/10.1016/j.heliyon.2023.e17401>

Received 17 January 2023; Received in revised form 15 June 2023; Accepted 15 June 2023

Available online 24 June 2023

2405-8440/© 2023 Published by Elsevier Ltd.

This is an open access article under the CC BY-NC-ND license

(<http://creativecommons.org/licenses/by-nc-nd/4.0/>).

lessening the speed of acute cellular rejection after solid organ transplantation.

In clinical practices, mAbs are extensively used as a biological product, which are developed and manufactured strictly following the international and regional guidance documents [12]. The desired product quality should be controlled and ensured through critical quality attributes (CQAs). CQAs include physical, chemical, biological, or microbiological properties or characteristics with an appropriate limit, range, or distribution. Potential drug substance CQAs are used to guide process development [13]. Therefore, the International Conference on Harmonization (ICH) Q6B has suggested guidelines for complex molecular agents such as mAbs, since the higher structure cannot be comprehensively and explicitly determined from physicochemical information but can be inferred from related biological activities. The biological activity of mAbs mainly depends on both Fab and Fc fragments. The traditional ELISA assay can give the information of binding ability between antibody and the target. However, the binding activity can not reflect the downstream reaction after the binding of antibody and target.

IL-2 not only exerts most of its effects on T lymphocytes but also participates in many pathophysiological roles, such as gene regulation and producing other cytokines such as TNF- α , by activating downstream signaling pathways. Therefore, a method which can reflect the complicated mechanism of action (MOA) of mAb should be developed to measure the bio-activities. Based on the experience obtained from our previous studies, a cell-based reporter gene assay (RGA) was capable to obtain the near-real biological activity through dose-dependent blockage of the downstream signaling pathways [14,15]. Herein, we constructed a T-lymphatic cell line C8166 that was stably transduced with a pLV-STAT5 RE-Luc-PGK-zeocin reporter gene to indicate the biological response in RGA assay [16,17] (the principle was shown in Fig. 1). We validated biological activity related parameters of specificity, linearity, precision, accuracy, and robustness [18,19] through optimizing conditions to evaluate the biological activity of related antibodies.

2. Materials and methods

2.1. Reagents and cell lines

RPMI-1640 medium containing GlutaMAX™, fetal bovine serum (FBS), and zeocin were purchased from GIBCO (USA). Recombinant human IL-2 (rhIL-2) was purchased from (Biotechnology). Cell culture flasks were purchased from Corning. Bright-Glo was purchased from Promega (USA). Commercialized antibody Basiliximab was obtained from Novartis (Basel, Switzerland) and preserved in our laboratory. T-lymphatic cell line C8166 (BNCC, BNCC339673) and human Hodgkin's lymphoma cancer cell line HDLM-2 (ATCC, CRL-2955) were cultured in RPMI-1640 medium.

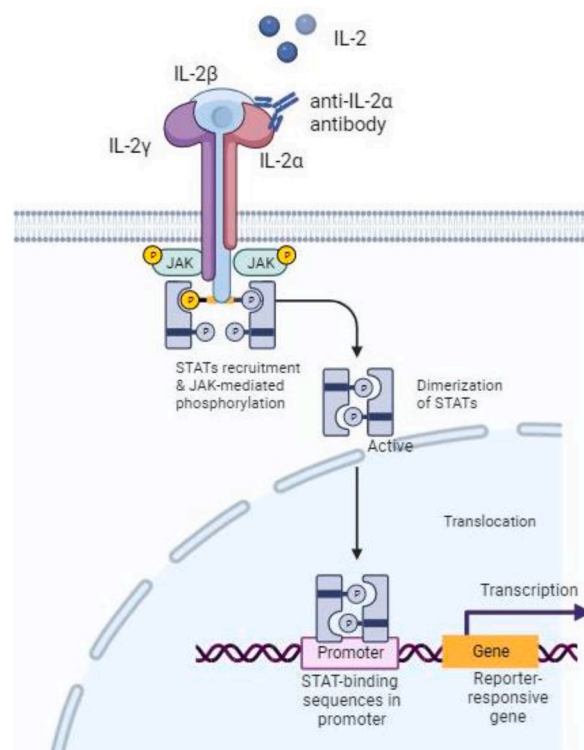


Fig. 1. Schematic diagram of IL-2/STAT5 reporter gene signal transductions and anti-IL-2 α antibody as an inhibitor.

2.2. Construction of plasmid and cell line generation

The full length of luciferase coding gene and five copies of STAT5 response element (AGTTCTGAGAAAAGT) with a minimal TATA-box promoter was amplified from pGL4.47 plasmid [luc2P/STAT5 RE/Zeocin] by PCR (forward primer: CGTCTAGATATTGGACAGGCCGCAATAAAATAT; reverse primer: CCACGCGTTTACACGGCGATCTTGCC). This PCR product was then cloned into plasmid pLV-CMV-PGK-zeocin (OBiO Technology, Shanghai, China) where the CMV promoter was displaced by MluI/XbaI digestion. To package the lentivirus of pLV-STAT5, RE-Luc was co-transfected with pCMV-dR8.2 and pCMV-VSV-G into HEK293T cells using lipofectamine (Thermo Fisher, USA). Two days later, cells were ultracentrifuged at $120,000\times g$ for 1.5 h at 4 °C, and the supernatant containing lentivirus was harvested. Subsequently, the lentivirus was integrated into the genome of C8166 cells and HDLM-2 cells to screen the stable cell clones expressing STAT5-actuated luciferase.

2.3. Flow cytometry analysis

IL-2R consists of three receptors: CD25, CD122, and CD132. To measure the expression of these three receptors in C8166 cells, C8166 cells (1×10^6 cells/mL) in 24-well plates were first harvested and washed twice with 1% BSA/PBS, resuspended with 1 mL of 1% BSA/PBS, and co-incubated for 60 min at 4 °C with 20 μg of FITC anti-CD25 antibody (Cat No.: 11025742, Thermo Fisher, USA), PE anti-CD122 antibody (Cat No.: 46122842, Thermo Fisher, USA), PE anti-CD132 antibody (Cat No.: 12132942, Thermo Fisher, USA) or the corresponding isotype control (Mouse IgG2b-FITC, CatNo.: 11473281; Mouse IgG1-PE, Cat No.: 46471482; Rat IgG2b-PE, Cat No.: 12403182, Thermo Fisher, USA), respectively.

To measure STAT5 phosphorylation, 1×10^6 C8166 cells for each test in 24-well plates were harvested and stimulated for 60 min at 37 °C with 10 ng doses of IL-2. The samples were then fixed and permeabilized with Intracellular Fixation & Permeabilization Buffer Set (Cat No.: 88882400, Thermo Fisher, USA) following the manufacturer's instructions and incubated for 60 min in 4 °C in different doses of PE anti-phospho-STAT5 (Tyr694) antibody (Cat No.: 12901042, Thermo Fisher, USA) and isotype control (Cat No.: 12471482, Thermo Fisher, USA), respectively. Finally, the cells were measured using a flow cytometer (BD FACSCalibur) and analyzed with FlowJo software (Flow Jo LLC, Ashland, OR, USA).

2.4. Selection of C8166-STAT5 RE-Luc cell clone

Five cells/mL, at a total of 50 mL, were cultured in 96-well transparent plates with 100 μL assay medium containing 50 $\mu g/mL$ zeocin (1640 medium containing GlutaMAX™ with 10% FBS) and cultured at 37 °C with 5% CO₂ for approximately 3–4 weeks. The selected cells were transferred to a 24-well plate and then transferred into a 25 mL culture flask. Cells (1×10^6 cells/mL in assay medium, 100 μL /well) and rhIL-2 (starting concentration of 500 ng/mL in 1:10 dilution ratio, 50 μL /well) were co-cultured in 96-well white plates. After 24 h of incubation, 50 μL of Bright-Glo luciferase assay reagent was added to each well. The relative light unit (RLU) values were recorded using an Envision bioluminescent reader system (PerkinElmer, USA).

2.5. RGA procedure

The assay medium of C8166-STAT5RE-Luc cells prepared with 1640 and 10%FBS. The viable cell density and viability should meet the requirement of 2.5×10^5 cells/mL and over 80% respectively. The cell suspension (100 μL /well in the density of 2.5×10^5 cells/mL) was added into 96-well white plates. Basiliximab was prepared at the initial concentration of 10 $\mu g/mL$, and serially diluted at a 1:3 ratio with medium containing 10 ng/mL IL-2. The diluted Basiliximab was transferred into 96 well plates with cells and incubated for 22 ± 2 h at 37 ± 2 °C, $5 \pm 1\%$ CO₂ and $\geq 85\%$ relative humidity. Bright-Glo (50 μL /well) was added and incubated at ambient temperature at least 2 min for reading.

2.6. Generation of force-degradation antibodies

Many factors affect the stability of antibodies during the development of therapeutic protein, such as temperatures, repeated freezing and thawing, and other factor. Basiliximab was heated in a water bath of 90 °C and 70 °C, respectively, for 10 min and treated by UV radiation for 24 h. Another set of samples from the same batch was heated in a water bath of 60 °C for 24, 72, 120, and 168 h. Basiliximab was repeatedly frozen and thawed once, twice, and three times at a low temperature at -80 °C. The above samples were processed for the bioactivity assay, which was run three times.

2.7. Size-exclusion chromatography

We performed size-exclusion chromatography (SEC) to gather data on the aggregates and fragments of proteins. Basiliximab was diluted in deionized pure water and assayed at the absorbance of 210 nm in high-performance liquid chromatography (HPLC), with the G3000SWXL (7.8 mm \times 30 cm, TSK, JP) as separation column and potassium phosphate (Cat No.: p5655 Sigma, GER) as mobile phase. Chromatography condition: Flow rate 0.4 mL/min, Detection UV, 210 nm Column temperature Ambient (25 ± 5 °C), auto-sampler temperature approximately 5 ± 3 °C, injection volume of 20 μL , and run time of 40 min.

2.8. Cation-exchange chromatography

We conducted charge heterogeneity analysis with cation-exchange chromatography (CEX) using the absorbance wavelength of 215 nm, using a ProPac WCX-100 column (4.0 mm × 250 mm, Cat No.: 054993, Thermo Fisher, USA) and with potassium phosphate (Cat No.: p5655, Sigma, GER) as mobile phase. We set 20 mM potassium phosphate, pH 6.0 as mobile phase A and 20 mM potassium phosphate, pH 6.0, containing 1 M potassium as mobile phase B. Samples were injected under conditions of 93% mobile phase A and 7% mobile phase B. A linear gradient from 7% mobile phase B to 16.5% at 57 min was initially applied. After 58 min, a linear gradient from 16.5% mobile phase B to 50% mobile phase B was applied to elute all proteins from the column. After 61 min, the column was returned to its original state using 70% mobile phase A and 30% mobile phase B for 10 min before the next injection.

2.9. Statistical analysis

All data were analyzed with GraphPad Prism 7.0 (GraphPad Prism, San Diego, CA, USA). The RLU value (y) and log-transformed concentrations of sample or standard reference (x) were fitted using a four-parameter equation ($y = (a - d)/[1 + (x/c)^b] + d$) to calculate the IC_{50} (half maximal inhibitory concentration) of sample or standard reference. The results of RGA assay depend on factors such as the state of the cells, the proficiency of the operators, and the types of key reagents and consumables, indicating that the IC_{50} values obtained in different individual tests do not have direct comparability. If it is necessary to accurately reflect the biological activity of the sample, the usual approach is to introduce a standard reference. The standard reference and the sample are tested under identical experimental conditions. The ratio of the IC_{50} value of the standard reference to the IC_{50} value of the sample is used as the relative activity of the sample. In this case, the results obtained by different laboratories and operators using the same method are only comparable. Hereinafter, we use relative potency to establish, optimize and validate the RGA method. In the above equation, coefficient a , d , b and c represent the maximum response (value from the y -axis) at the upper asymptote, the minimum response (value from the y -axis) at the lower asymptote, the slope of the concentration response curve between the lower and upper asymptotes, and the IC_{50} at which 50% of the response is generated at concentration x , respectively.

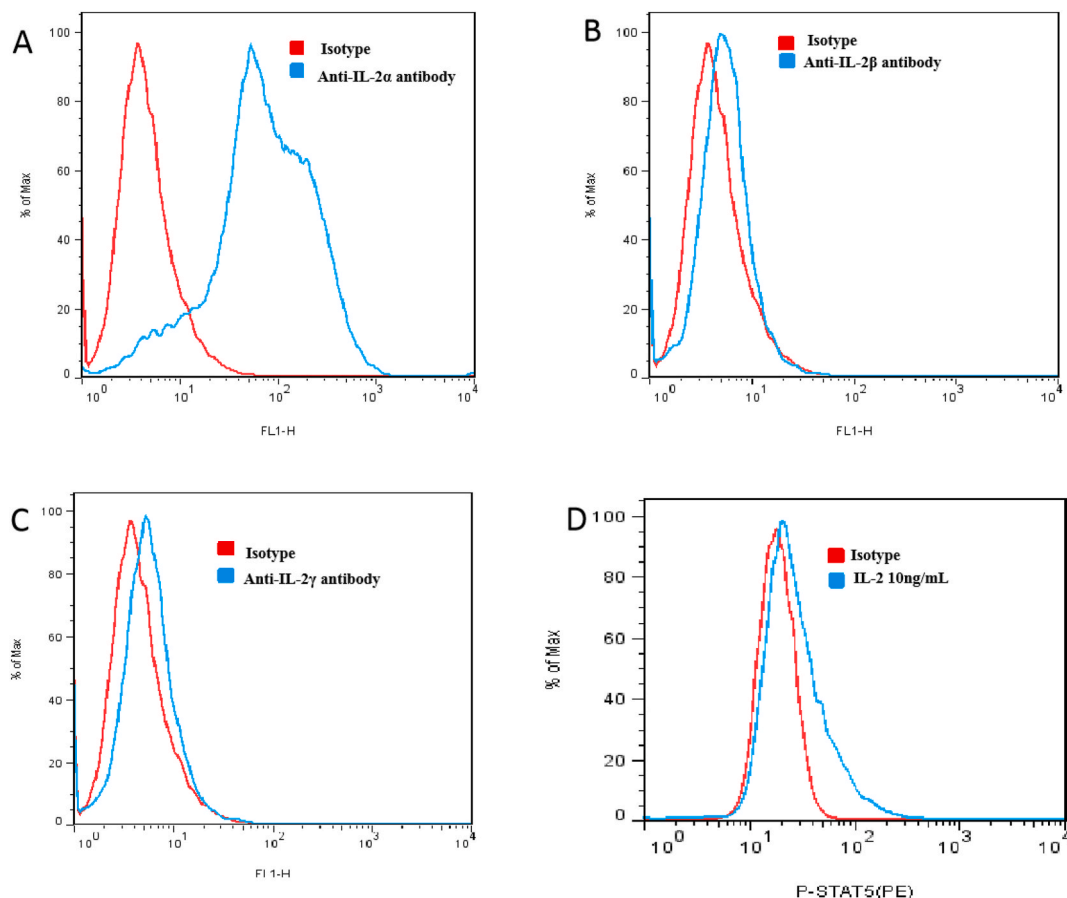


Fig. 2. Generation of C8166/STAT5-luc cells. Flow cytometry analysis of IL-2R α (A), IL-2R β (B), and IL-2R γ (C) expression on the cell membranes of C8166 cells. (D) IL-2 at a concentration of 10 ng/mL was incubated with C8166 cells and flow cytometry was used to assess the binding ability of IL-2 to cells.

3. Results

3.1. Generation of IL-2-responsive C8166-STAT5 RE-Luc cell line

To establish a stable IL-2-responsive cell line, C8166 cells were transduced with STAT5-Luc lentiviral particles. Flow cytometry was used to confirm the expression IL-2R on the surface of C8166 cells (Fig. 2A, B, and 2C). Subsequently, flow cytometry was also used to measure intracellular STAT5 phosphorylation in C8166 cells after stimulated by IL-2 for 60 min (Fig. 2D), which served as a proof of concept for the RGA design. Phosphorylated STAT5, in C8166-STAT5RE-Luc, that was related with intranuclear STAT5 was able to activate luciferase transcription.

HDLM-2 cells highly expressed IL-2R and were also transduced with STAT5-Luc lentiviral particles, but had low RLU signals (Fig. 3A). The RLU signals were recorded to analysis the highest value and the lowest value ratio as signal-to-noise ratio (S/N). The monoclonal in the well whose position was the eighth column of row C of the third 96-well plate were named as clone 3C8 by an optimal S/N. This cell serves as master cell bank for the process of validation (Fig. 3B).

3.2. Optimization of the condition in the bioassay

Adhering to the principle of keeping a single variable in an experiment to optimize major conditions, we adjusted incubation time, cell density, IL-2 concentration, initial Basiliximab concentration and dilution ratio, and FBS concentration.

First, incubation times of clone 3c8 (C8166 transduced with STAT5-luc gene) were tested via S/N at 6, 8, 15, 17, 20, 24, and 36 h respectively. The RLU was used to describe the intensity of signal from transgenic cells (Fig. 4A). The optimal incubation time was determined to be 24 h in terms of time and S/N (Fig. 4B). Cell density was also found to be a significant factor influencing the curves due to the number of receptors present. We tested 5.0×10^3 , 2.5×10^4 , 5.0×10^4 , and 1.0×10^5 cells/well in the detection and found that 2.5×10^4 cells/well were optimal (Fig. 4C and D).

Subsequently, intracellular STAT5 phosphorylation is activated and a downstream signaling cascade is stimulated when IL-2 binds to the receptor. Therefore, the IL-2 concentration is another critical factor. A primary concentration of IL-2 of 40 ng/mL, according to the IL-2 effective concentration curve, was used to select a proper antigen stimulation of concentration such as 100, 50, 20, 10, 5, and 2 ng/mL. Basiliximab was serially diluted (1:5) to acquire a dose-response curve. Although four-parameter curves had different S/N ratios, the optimal S/N ratios were obtained when the concentrations of IL-2 were 10 ng/mL and 20 ng/mL (Fig. 5A). The final concentration of IL-2 was determined to be 10 ng/mL considering the cost saving.

Finally, the concentration of IL-2 was determined to be 10 ng/mL as antigen by using a series of dilutions. In this case, an inhibition curve including rich points on the upper and lower asymptotes was obtained (Fig. 5B). To ensure that the points were uniformly distributed, dilution ratios of 1:2, 1:3, 1:4, 1:5, and 1:6 were tested to obtain a series of curves (Fig. 5C). The dilution ratio of 1:3 was selected as a condition in subsequent experiments. FBS is a critical external condition, and results showed that 10% FBS was the best concentration (Fig. 5D). By optimizing the above parameters, we obtained a best-fit sigmoidal curve of Basiliximab for this bioassay. The summary of the optimization parameters is shown in Table 1, which was used in the following experiments.

3.3. Validation of the RGA

A bioassay needs to be validated for specificity, linearity, accuracy, precision, and robustness based on the ICH Q2 (R1) guidelines and the *Chinese Pharmacopoeia*. Specificity can be shown by demonstrating that the identification and quantitation of an analyte is not impacted by the presence of other substances (e.g., impurities, degradation products, related substances, being repeatedly frozen and

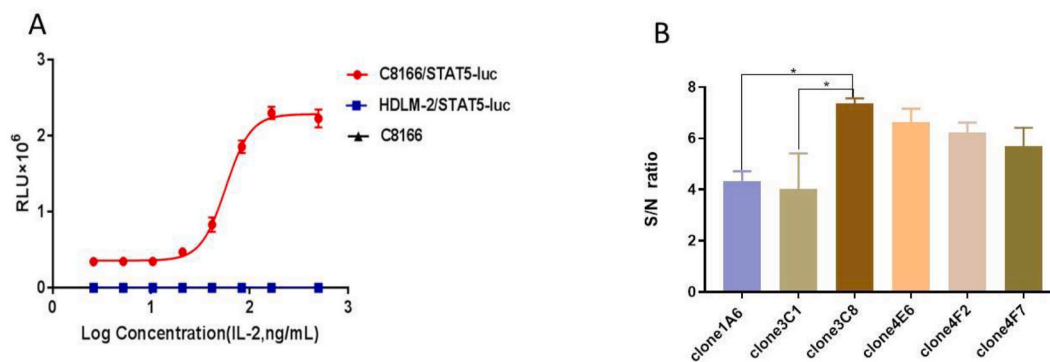


Fig. 3. (A) HDLM-2 cells transduced with the pLV-STAT5-Luc-PGK-zeocin reporter gene were stimulated with IL-2 at an initial concentration of 500 ng/mL, with a 1:3 dilution ratio. RLU was measured after adding 50 μ L/well Bright-Glo per well. Non-transduced C8166 cells were used as negative control, and the signal-to-noise ratio (S/N) of luminescence response was not detected. Only C8166 cells transfected with the pLV-STAT5RE-Luc-PGK-zeocin reporter gene stimulated with IL-2 had a dose relationship. (B) The clone 3c8 was compared to other clones, and had an optimal S/N and 50% effective concentration (EC_{50}). The error bars represent the mean \pm SD from three repeated assays, * $p < 0.05$.

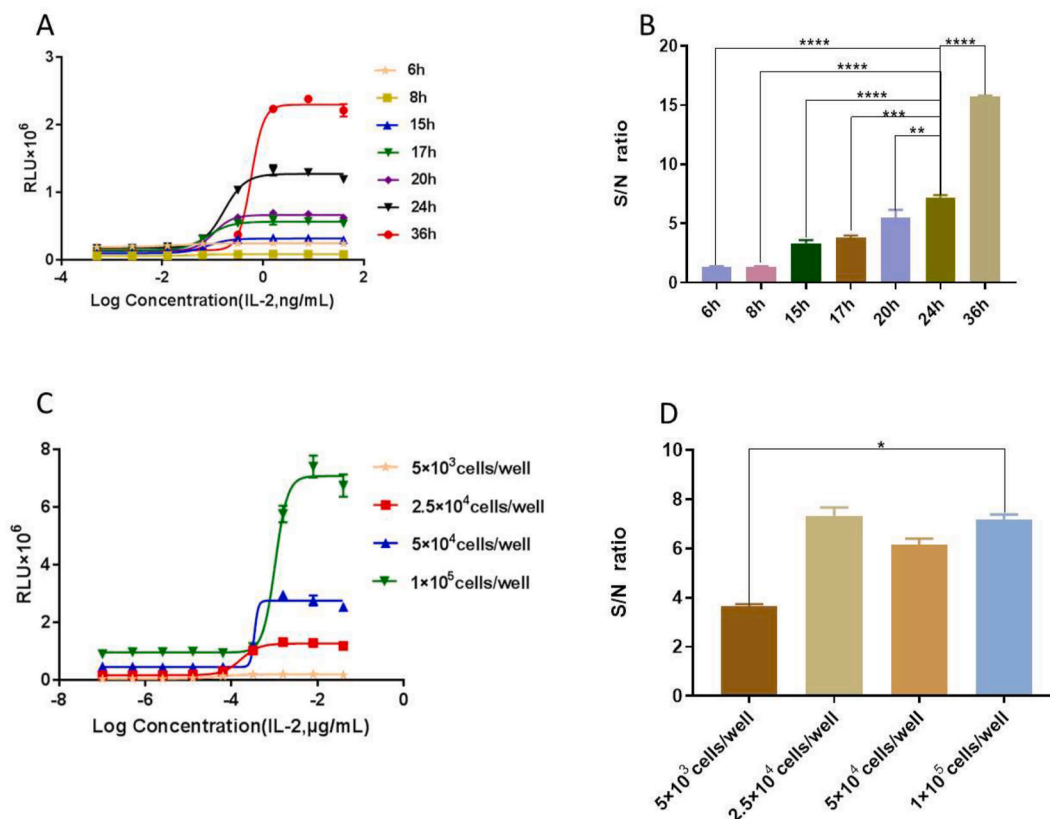


Fig. 4. Optimization of incubation time and cell density used in the RGA assay. (A) Clone 3c8 cells ($100 \mu\text{L}/\text{well}$ at the density of 2.5×10^6 cells/mL) were co-cultured with serially diluted rhIL-2 ($50 \mu\text{L}/\text{well}$ with the initial concentration of 40 ng/mL and 1:5 dilution ratio) and incubated for 6, 8, 15, 17, 20, 24, and 36 h, respectively. Four-parameter curves displayed the relationship between log-transformed rhIL-2 concentration and RLU. (B) RM one-way ANOVA and Dunnett's multiple comparisons test was used to statistically compare the S/N values obtained at different incubation times. (C) Clone 3c8 cells were prepared with initial density of 1×10^5 cells/well/ $100 \mu\text{L}$ and 1:5 dilution ratio, followed by co-cultured with serially diluted rhIL-2 ($50 \mu\text{L}/\text{well}$ with the initial concentration of 40 ng/mL and 1:5 dilution ratio) and then incubated for 24 h. (D) RM one-way ANOVA and Dunnett's multiple comparisons test was used to statistically compare the S/N values obtained at different cell density. Notes: The points and error bars showed on the curves and histograms represent the mean values and standard deviations from three repeated assays. The asterisk means * $p < 0.05$, ** $p < 0.01$, *** $p < 0.001$, **** $p < 0.0001$.

thawed, matrix, or other components present in the operating environment). The linearity between sample concentration and response should be evaluated across the working range of the analytical procedure to confirm the suitability of the procedure for the intended use. Accuracy should be established across the reportable range of an analytical procedure and is typically demonstrated through comparison of the measured results with the expected results. Precision should be investigated using homogeneous, authentic samples or artificially prepared samples. Precision should include repeatability, intermediate precision and reproducibility [20–22]. Robustness testing should show the reliability of an analytical procedure with respect to deliberate variations in parameters.

3.3.1. Specificity of the RGA

Specificity describes the ability to assess the analyte of relevance and the ability to distinguish between other irrelevant analytes. In this study, unrelated IL-2 mAbs such as Tocilizumab (the relative bioactivity was 98% using BaF cell proliferation inhibition method), Cetuximab (the relative bioactivity was 120% using DiFi cell proliferation inhibition method), Ustekinumab (the relative bioactivity was 109% using NK92MI cell binding activity), and Ixekizumab (the relative bioactivity was 109% using NK92MI cell binding activity) had no dose-response curves. Anti-CD25 recombinant human mAbs from other manufacturers have similar dose-response curves to Basiliximab (Fig. 6A). Flow cytometry method was used to determine the relative bioactivity of related IL-2 mAbs such as Basiliximab (100%) and Anti-CD25 rhmAb (92%), respectively.

IL-2R is a heterotrimeric protein with CD25, CD122 and CD132 expressed on the surface of certain immune cells. We further found anti-CD122 antibody and anti-CD132 antibody displayed dose-response inhibitory activities (Fig. 6B). Forced degradation was also used to evaluate the specificity of RGA. First, Basiliximab was repeatedly frozen and thawed for one, two, and three cycles. The processing method did not make a difference on the bioassay of Basiliximab, confirming the stability this product (Fig. 6C). Subsequently, we assessed the effect of temperature on product stability. Basiliximab was divided into four tubes, and each tube was placed in a 60°C water bath for 24, 72, 120, or 168 h, which was detected using the RGA bioassay. Our findings clearly show a declining trend

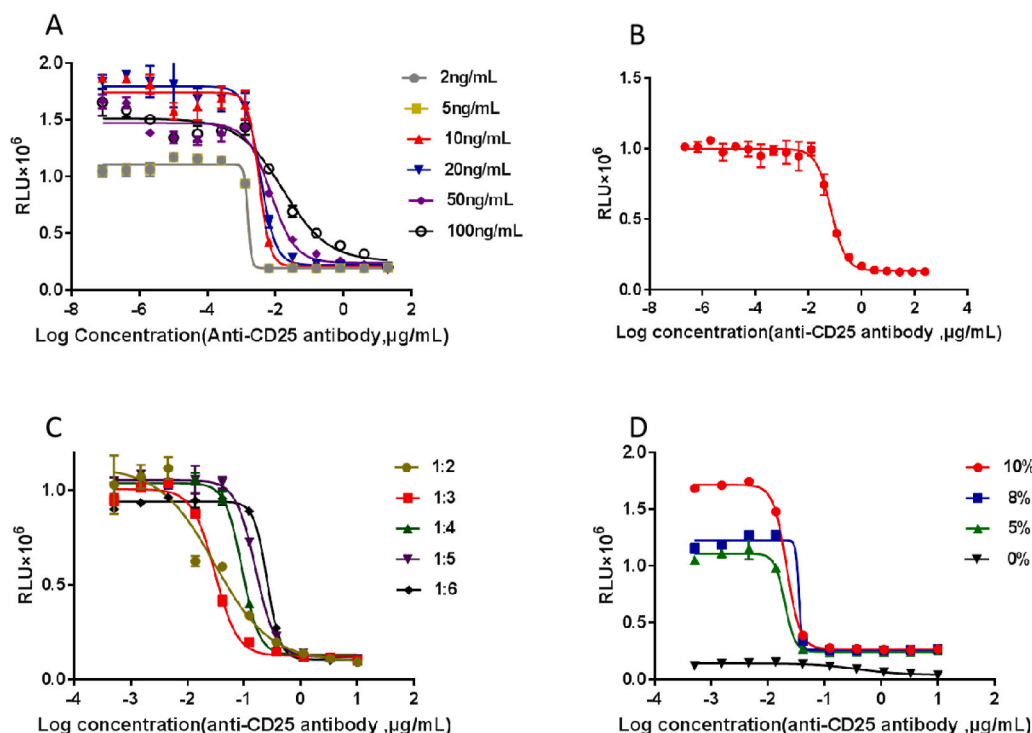


Fig. 5. Optimization of RGA conditions. (A) Six IL-2 concentrations were seeded to be inhibited by diluted Basiliximab (starting concentration 40 $\mu\text{g}/\text{mL}$, dilution ratio 1:5). (B) Exploration of starting concentration of Basiliximab, according to an incubation time of 24 h and 2.5×10^4 cells/well, a Basiliximab concentration of 250 $\mu\text{g}/\text{mL}$ at 1:5 dilution ratio was diluted in 10 ng/mL IL-2 to obtain inhibition curves. (C) The starting concentration of Basiliximab was 10 $\mu\text{g}/\text{mL}$; the primary concentration of IL-2 was 10 ng/mL; dilution ratios of 1:2, 1:3, 1:4, 1:5, and 1:6 were used to create five inhibition curves; and C8166-STAT5 RE-Luc cells were incubated for 24 h. The full 10 points were used to fit the four-parameter model. Through the best-fit curve having rich points on the upper and lower asymptotes, 1:3 was found to be the best dilution ratio. (D) Optimization of concentration of FBS was performed. Different concentrations of FBS (0%, 5%, 8%, and 10%) were tested according to the stated conditions, and four inhibition curves were obtained. The error bars represent the mean \pm SD from three repeated assays.

Table 1
Optimal conditions of main parameters for RGA assay.

| Experimental parameter | Optimal condition |
|---------------------------------------|------------------------------|
| Starting concentration of Basiliximab | 10 $\mu\text{g}/\text{mL}$ |
| Serial dilution ratio of Basiliximab | 1:3 |
| IL-2 concentration | 10 ng/mL |
| Cell density | 2.5×10^4 cells/well |
| Incubation time | 24 h |

that strongly demonstrates the specificity of RGA (Fig. 6D). Finally, different processing methods were tested in the treated product, and the IC_{50} was calculated to compare with the untreated product. Accelerated degradation treatments include UV radiation, 70 $^{\circ}\text{C}$ and 90 $^{\circ}\text{C}$ incubation, which had a great impact on bioactivity (Fig. 6E and F). Conclusively, these alterations of bioassay on bioactivity were successfully evaluated. The results are calculated by a four-parameter equation ($y = (a - d)/[1 + (x/c)^b] + d$).

IL-4 signalings through the STAT5 and STAT6 pathways [23,24], IL-6 signals through the STAT3 and STAT5 pathways and rh-GSF signals through the STAT1, STAT3 and STAT5 signaling pathways [25–29]. IL-4, IL-6 and rh-GSF share the same signaling pathway, i. e., STAT5. They have no dose-response curves in the constructed cells (Fig. 7).

Bioassays are vital to assess product stability and can reflect the high-level structure of numerous quality control indicators. To further evaluate the specificity of the RGA under the circumstances of forced degradation, SEC-HPLC and CEX-HPLC were used to detect aggregates and fragments (Fig. 8A and B). Aggregates and fragments of related products were increased using the different forced degradation methods, as determined via SEC-HPLC. Degradation products were increased using different forced degradation methods, as determined via CEX-HPLC. There were corresponding changes in the biological activity. These two physical and chemical experiments further confirmed the sensitivity and accuracy of RGA.

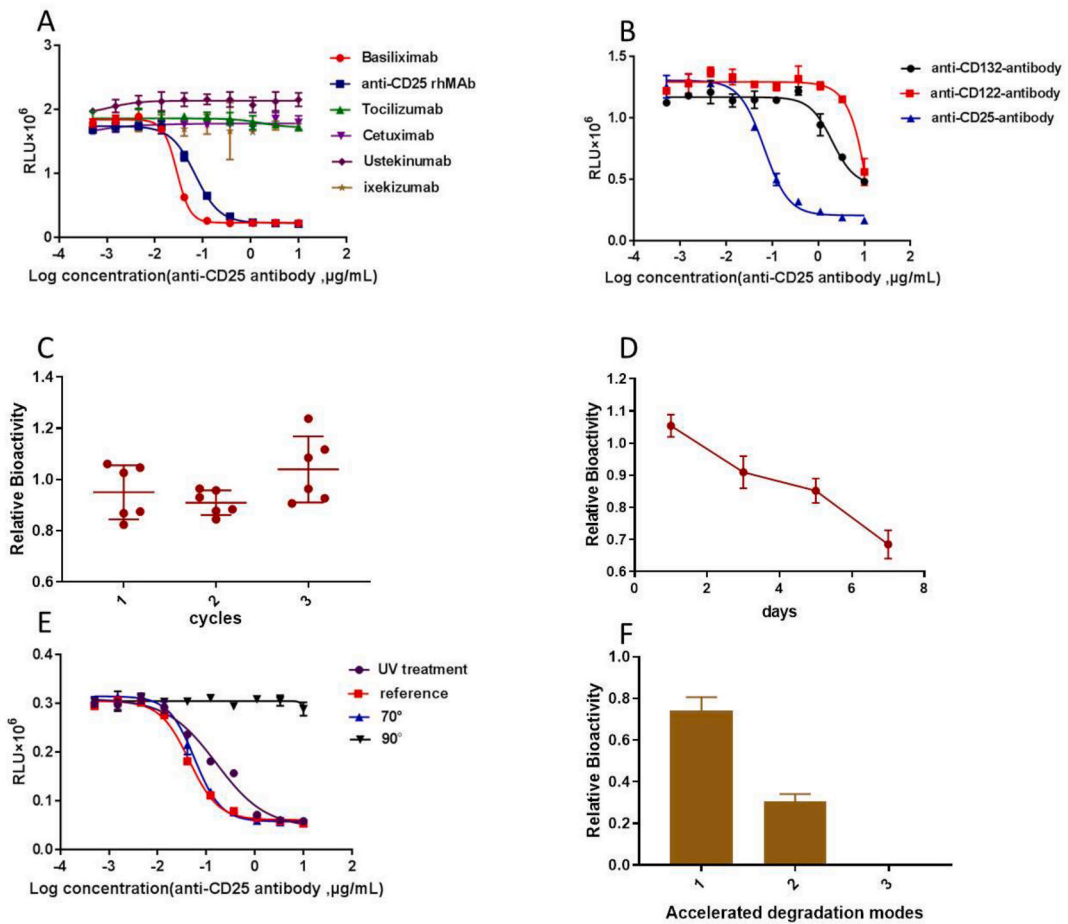


Fig. 6. The specificity validation of RGA. (A) Six curves of different mAbs were obtained with C8166-STAT5RE-Luc cells using the same conditions. (B) Three curves of different mAbs were obtained with C8166-STAT5RE-Luc cells using the same conditions. (C) One cycle of relative bioassay of Basiliximab was detected with 82–106%. Two cycles of relative bioassay of Basiliximab were detected with 86–96%. Three cycles of relative bioassay of Basiliximab were detected with 93–124%. (D) Different times to treat Basiliximab of relative bioassay at 60 °C were detected with 102–109% (24 h), 86–96% (72 h), 81–89% (120 h), 64–74% (168 h) bioactivity. (E) The treatment of Basiliximab was detected at 70 °C for 10 min (67–79%), with UV treatment for 48 h (28–35%) and at 90 °C for 10 min (0%). (F) The stability of Basiliximab is affected by different methods of accelerated degradation. The 1st sample was at 70 °C for 10 min, the 2nd with UV treatment for 24 h, and the 3rd at 90 °C for 10 min. The error bars represent the mean ± SD from three experiments.

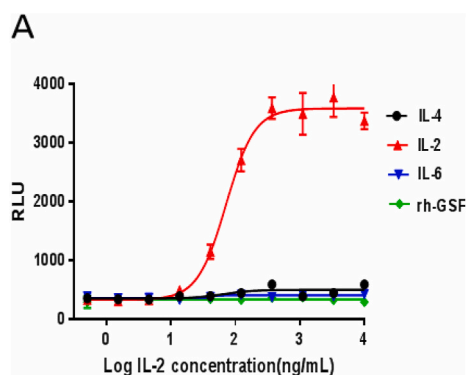


Fig. 7. Four curves of different molecules were obtained with C8166-STAT5RE-Luc cells using the same conditions.

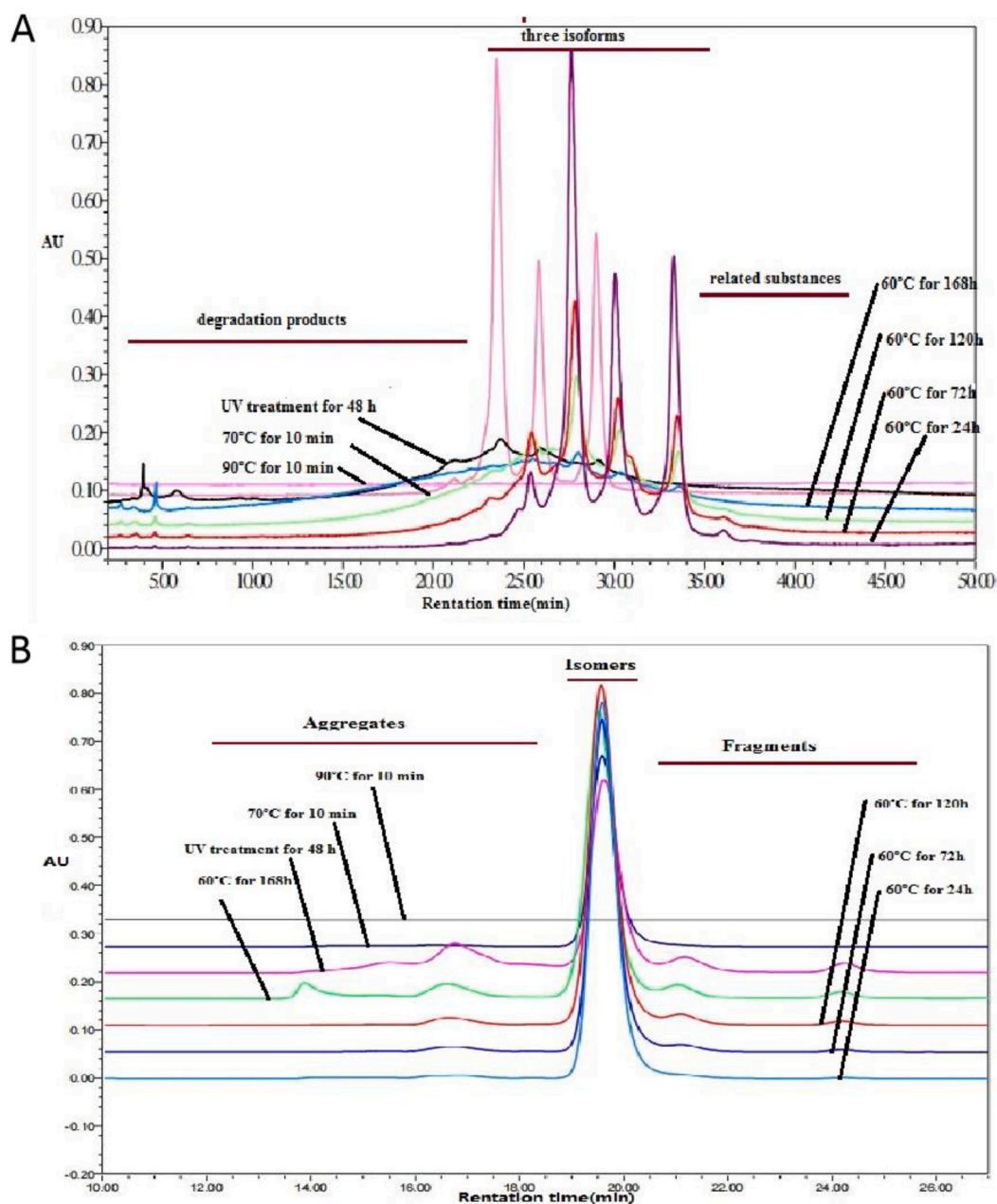


Fig. 8. (A) Different samples processing methods were acquired using data from charge isomers of CEX. Accessory and degradation substances were greatly changed by the different forced degradation methods as determined by CEX-HPLC, with the increase of accessory and degradation substance leading to a decrease in bioactivity. (B) Different samples processing methods were analyzed by size isomers using SEC. Different methods of processing samples were acquired using data from size isomers of SEC. Both the high weight molecules (HWM) and low weight molecules (LWM) were greatly changed using the different forced degradation methods as determined by SEC-HPLC, with the increase of HWM and LWM leading to a decrease in bioactivity.

3.3.2. Accuracy and linearity of the RGA

It was directly inferred that the linear curve between the measured and expected values also showed excellent linearity with R^2 as indicator. Here, the reference standard of Basiliximab was diluted to 50%, 75%, 100%, 125%, and 150%, respectively, as five samples to be tested. Through RGA assay, the measured values (y) and expected values (x) were compared and they is a linear correlation between the two fitted that the linear curve ($y = 0.948x + 8.6$) between the measured and expected values also showed linearity with R^2 equals to 0.9936, that is, $y = 0.948x + 8.6$, within the range of 50–150%, " (expected potency = measured potency - 0.86)/0.948" holds a quadratic linear relationship with range (Fig. 9A).

To measure if the relative potency was close to the true or reference standard within a reasonable range (80–125%), five

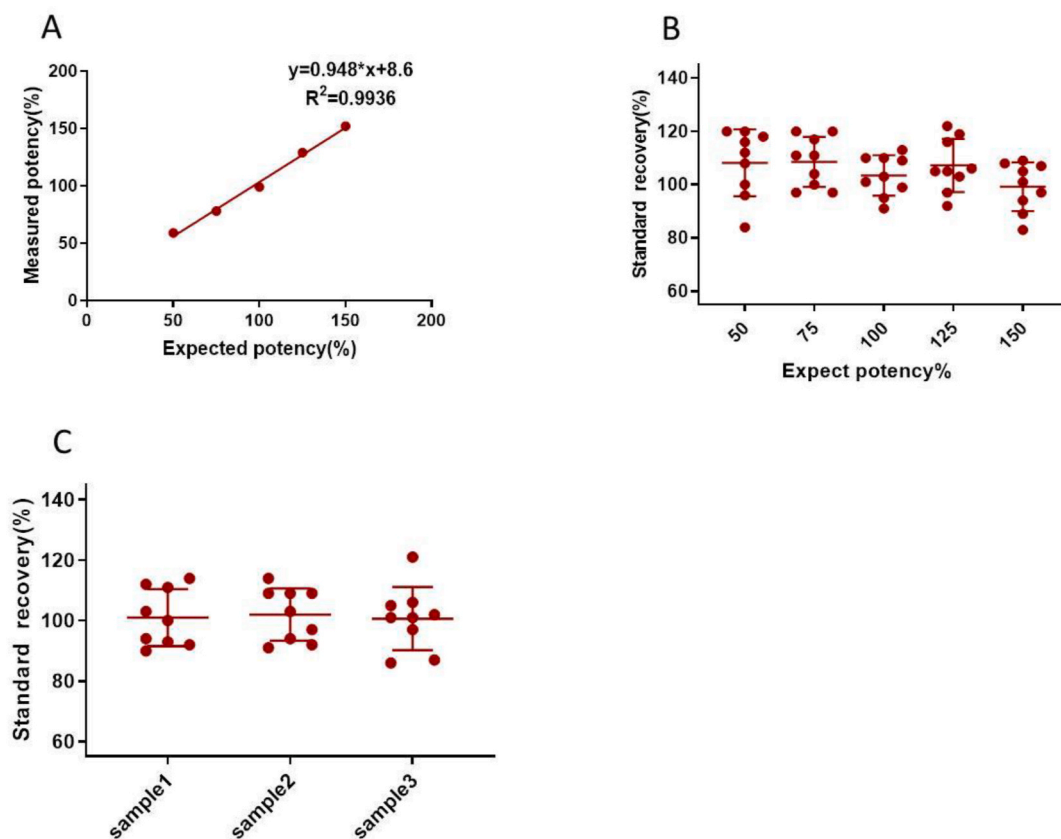


Fig. 9. The linearity and accuracy validation of RGA. (A) The expected and measured potency of bioactivity had a high correlation in 50–150%. These detected data were repeated nine times. (B) 50, 75, 100, 125, and 150% of Basiliximab from the optimized primary points were detected using the RGA; the relative potency was in the range of 84–120% applied to individual values. (C) Three different batches of Basiliximab were mixed with equal volumes of reference sample and the reference recovery was in the range of 86–120%. The error bars represent standard deviation (SD). The results are calculated by a four-parameter equation ($y = (a-d)/[1 + (x/c)^b] + d$). The error bars represent the mean \pm SD from three experiments.

concentrations including 50%, 75%, 100%, 125%, and 150% were tested when all other conditions were kept constant. Simultaneously, Basiliximab was detected using the optimized conditions on the same 96-well plate as the reference standards. The titer of reference standard was calculated as IC_{50} . The recovery rate of 50% reference standard = (the measured results of 50% reference standard - 50% \times the measured results of 100% reference standard)/50%. All the samples were detected nine times to calculate the recovery rate. The IC_{50} values of the five samples were calculated using the ratio to the reference (Relative potency of sample = IC_{50} of reference standard/ IC_{50} of sample \times 100%), and all the samples were detected nine times (Fig. 9B).

The recovery is vital to assess the accuracy of RGA assay. Specifically, the drug substance has a different set of ingredients in the buffer system with drug products. We detected a reference recovery of equal volume by mixing a reference and the sample. Three different batches of samples were selected to detect recovery (Fig. 9C).

3.3.3. Precision of the RGA

A batch of Basiliximab was assessed for repeatability of intra-day, inter-day, and different analysts by calculating the relative

Table 2

The precision and intermediate precision of Basiliximab's relative bioactivity using RGA.

| | | 1 | 2 | 3 | 4 | 5 | 6 | Precision | | |
|------------------------|------|-------|--------|--------|--------|--------|--------|-----------|------|------|
| | | | | | | | | Mean | SD | CV% |
| 1 | | 84.18 | 97.22 | 95.04 | 94.62 | 89.7 | 108.67 | 94.9 | 8.21 | 8.65 |
| 2 | | 105.5 | 107.3 | 108.77 | 103.33 | 108.74 | 110.28 | 107.32 | 2.53 | 2.36 |
| 3 | | 93.93 | 102.43 | 91.23 | 89.71 | 84.87 | 85.83 | 91.33 | 6.4 | 7.01 |
| Intermediate precision | Mean | 97.85 | | | | | | | | |
| | SD | 9.14 | | | | | | | | |
| | CV% | 9.34 | | | | | | | | |

bioactivity. Six experiments were performed by different analysts on the same day, with each analyst conducting the experiment on different days. Precision and intermediate precision were expressed by the coefficient of variation (CV%) (Table 2). All of the values were in the range of 84–110%. Both the precision (intra-day CV%) and intermediate precision (inter-day CV%) were no more than 10%. Moreover, the mean relative bioactivity was 102% for analyst A and 99% for analyst B. These data show that RGA used for assessment of biological activities of Basiliximab was sufficiently repeatable and precise. The results are calculated by a four-parameter equation ($y = (a - d) / [1 + (x/c)^b] + d$).

3.3.4. Robustness of the RGA

We assessed the stability of the C8166-STAT5RE-Luc cell line. Three different cell passages (13, 24, and 39) were cultured to verify the robustness of RGA. These cell passages were simultaneously used to assess the bioactivities of Basiliximab from the identical batch. There were no statistical differences in the three cell passages for the dose dependent curves in Fig. 10B and S/N ratios as shown in Fig. 10A. This result confirms that the RGA is stable for cells up to passage 39.

4. Discussion

Basiliximab has been proved to reduce the incidence of acute rejection episodes after renal transplantation. It is a recombinant murine and human chimeric IgG1 mAb binding to a specific epitope on IL-2R α in the seven amino acids string E-R-I-Y-H-F-V at positions 116–122 in the extracellular domain of the α -chain. This includes the IL-2 contact sites at three amino acids I–Y–H (positions 118–120) [30]. Basiliximab specifically binds to CD25 to inhibit IL-2-mediated proliferation of T lymphocytes. This is a pivotal step in the cellular immune response involved in allograft rejection. Furthermore, Basiliximab also binds to macrophages and monocytes.

As a biological product with complex structure and function, a MOA related bioassay was crucial for evaluating the efficacy of Basiliximab. To realize it, an in vitro cell line naturally expressing IL-2R on the surface is essential. C8166 and HDLM-2 cells highly expressed IL-2R were selected as candidates. Except for capturing the mAb by expression of IL-2R, the detection of the activated downstream signaling is required. Based on the evidenced signaling pathway, a luciferase gene in the control of STAT5 elements was stably transduced into the cell line. T lymphocyte cell line, C8166, was established from T cell lymphoma in patients with leukemia. The proliferation of C8166 cell is mediated by an autocrine pathway involving endogenous IL-2 production and its binding to cell surface receptors [31–32]. In theory, the luciferase gene should be expressed and can be detected once IL-2 binds to IL-2R on the cell, but the response will be blocked when adding Basiliximab and the response should be dose-dependent. The data in our study proved the feasibility of C8166-STAT5RE-luc cell line used in the biological activity assay of anti-CD25 mAbs. But unfortunately, another IL-2R-expressed cell line HDLM-2 failed to act as target cells [34–36], due to relative low basal levels of phosphorylation compared to other cell lines.

Based on the C8166-STAT5RE-luc cell line, we developed a highly sensitive RGA that was able to detect blocking of IL-2 binding to the receptor CD25 by Basiliximab. In accordance with ICH Q2-R1 guidelines and *Chinese Pharmacopoeia* requirements, the parameters such as density of cells, dilution ratio, incubation time, and initial concentration of the RGA were explored and optimized to evaluate the RGA of Basiliximab. Results showed that the RGA assay has excellent precision, accuracy, and high correlation with downstream reaction mechanisms, which can be applied in the quality control of biotechnology drugs [36]. The C8166-STAT5RE-Luc reporter gene cell line was responsive to anti-CD122 and anti-CD132 antibodies (Fig. 4B). In the research and development process, the cell line can be applied to bioassay detection for relevant targets. HEK293-based RGA for detecting the biological activity of anti-CD25 mAbs has already been developed, but the HEK293 cell line was simultaneously transfected with four different plasmids to express three receptors and a reporter. In contrast, IL-2R heterotrimer naturally expressed on the surface of C8166 cell line and IL-2/IL-2R binding is the intrinsic signaling start. Therefore, C8166 based RGA has advantages in reflecting the MOA of IL-2 and anti-CD25 mAbs, when compared to the previously reported HEK293 based RGA.

Basiliximab is produced as a lyophilized powder, which ultimately improves product manufacturability, delivery of the drug, storage stability, and administration to the patient. During the lyophilization process, lyoprotectants are essential during freezing and drying, as well as throughout storage to protect the mAbs. Sucrose, glycine, and mannitol are contained in the current landscape of excipients used in marketed biological products [37,38]. The reference standard of Basiliximab is provided in a liquid formulation. We evaluated the effect of lyophilization on the product's biological activity through the recovery rate. Results proved that the range of the recovery rate of the reference standard is within a reasonable and effective range. Moreover, multiple attributes of the antibody were evaluated, including charge heterogeneity by CEX–HPLC and purity by SEC–HPLC to evaluate the product of forced degradation. Accessory and degradation substances were greatly changed by the different forced degradation methods as determined by CEX–HPLC (Fig. 9A). Aggregates and fragments increased using the different forced degradation methods, as determined by SEC–HPLC (Fig. 9B). These results of quality attributes were compliant with our RGA. Furthermore, these results prove that the RGA was accurate and precise [39].

In conclusion, the C8166-STAT5RE-Luc reporter gene cell line was successfully constructed by transducing with lentiviral particles to detect the biological activity of anti-CD25 mAbs. It showed adequate performance in the bioassay to conduct quality control of anti-CD25 mAbs. The RGA provides a novel method to evaluate developed antibodies drugs that specifically target IL-2 in the future.

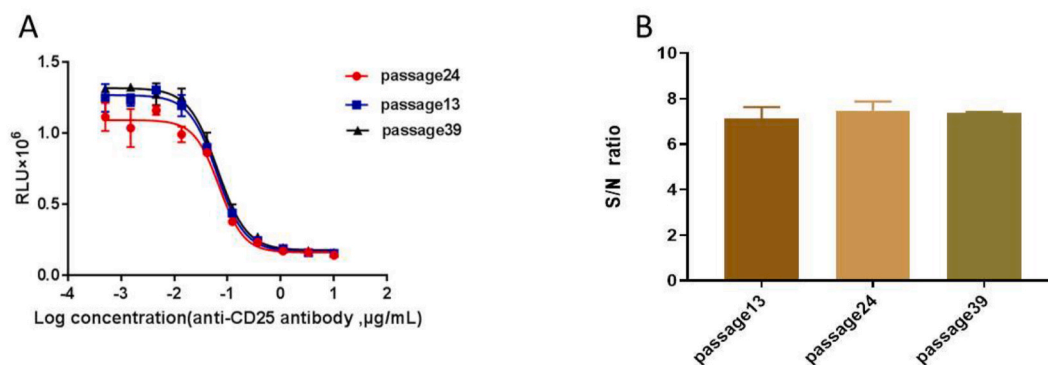


Fig. 10. The robustness validation of RGA. (A) C8166-STAT5RE-luc cells were simultaneously detected by the optimized RGA by plotting dose-dependent curves of 13, 24, and 39 cell passages in response to Basiliximab. (B) The S/N ratio of three different passages of C8166-STAT5RE-luc cells was shown. The results are calculated by a four-parameter equation ($y = (a-d)/[1 + (x/c)^b] + d$). The error bars represent the mean \pm SD from three repeated assays.

Declarations

Author contribution statement

Maoqin Duan, Chuanfei Yu, Yalan Yang: Conceived and designed the experiments; Performed the experiments; Analyzed and interpreted the data; Wrote the paper.

Maoqin Duan, Chuanfei Yu: Conceived and designed the experiments; Wrote the paper.

Zhihao Fu, Chunyu Liu, Jialiang Du, Meng Li: Performed the experiments.

Sha Guo, Xiaojuan Yu: Analyzed and interpreted the data.

Gangling Xu, Yuting Mei: Contributed reagents, materials, analysis tools or data.

Lan Wang: Conceived and designed the experiments; analyzed and interpreted the data; Contributed reagents, materials, analysis tools or data; Wrote the paper.

Funding statement

Lan Wang was supported by Ministry of Science and Technology of China [2019ZX09732-002].

Data availability statement

Data included in article/supp. material/referenced in article.

Declaration of competing interest

The authors declare that they have no known competing financial interests or personal relationships that could have appeared to influence the work reported in this paper.

References

- [1] V.A. Rao, J.J. Kim, D.S. Patel, K. Rains, C.R. Estoll, A comprehensive scientific survey of excipients used in currently marketed, therapeutic biological drug products, *Pharm. Res-Dordr* 37 (2020) 200, <https://doi.org/10.1007/s11095-020-02919-4>.
- [2] S. Guo, C. Yu, Y. Wang, F. Zhang, J. Cao, C. Zheng, L. Wang, A robust and stable reporter gene bioassay for anti-IgE antibodies, *Anal. Bioanal. Chem.* 412 (2020) 1901–1914, <https://doi.org/10.1007/s00216-020-02442-w>.
- [3] J. Mock, C. Pellegrino, D. Neri, A universal reporter cell line for bioactivity evaluation of engineered cytokine products, *Sci. Rep. -UK* 10 (2020) 3234, <https://doi.org/10.1038/s41598-020-60182-4>.
- [4] C. Yu, F. Zhang, G. Xu, G. Wu, W. Wang, C. Liu, Z. Fu, M. Li, S. Guo, X. Yu, L. Wang, Analytical similarity of a proposed biosimilar BVZ-BC to bevacizumab, *Anal. Chem.* 92 (2020) 3161–3170, <https://doi.org/10.1021/acs.analchem.9b04871>.
- [5] J. Sageshima, G. Ciancio, L. Chen, G.R. Burke, Anti-interleukin-2 receptor antibodies-basiliximab and daclizumab-for the prevention of acute rejection in renal transplantation, *Biol. Targets & Ther.* 3 (2009) 319–336, <https://doi.org/10.2147/btt.2009.3257>.
- [6] V. Duprez, G. Lenoir, A. Dautry-Varsat, Autocrine growth stimulation of a human T-cell lymphoma line by interleukin 2, *P NATL ACAD SCI USA* 82 (1985) 6932–6936, <https://doi.org/10.1073/pnas.82.20.6932>.
- [7] T. Woehrle, C. Ledderose, J. Rink, C. Slubowski, W.G. Junger, Autocrine stimulation of P2Y1 receptors is part of the purinergic signaling mechanism that regulates T cell activation, *Purinerg Signal* 15 (2019) 127–137, <https://doi.org/10.1007/s11302-019-09653-6>.
- [8] K. McKeage, P.L. McCormack, Basiliximab: a review of its use as induction therapy in renal transplantation, *BioDrugs* 24 (2010) 55–76, <https://doi.org/10.2165/11203990-000000000-00000>.

- [9] J. Huang, L. Wang, C. Yu, Z. Fu, C. Liu, H. Zhang, K. Wang, X. Guo, J. Wang, Characterization of a reliable cell-based reporter gene assay for measuring bioactivities of therapeutic anti-interleukin-23 monoclonal antibodies, *Int. Immunopharmacol.* 85 (2020), 106647, <https://doi.org/10.1016/j.intimp.2020.106647>.
- [10] A. Wallace, S. Trimble, J.F. Valliere-Douglass, M. Allen, C. Eakin, A. Balland, P. Reddy, M.J. Treuheit, Control of antibody impurities induced by riboflavin in culture media during production, *J. Pharm. Sci. US* 109 (2020) 566–575, <https://doi.org/10.1016/j.xphs.2019.10.039>.
- [11] J. Yuan, J. Li, L. Yang, Y. Lv, C. Wang, Z. Jin, X. Ni, H. Xia, Development and validation of a novel reporter gene assay for determination of recombinant human thrombopoietin, *Int. Immunopharmacol.* 99 (2021), 107982, <https://doi.org/10.1016/j.intimp.2021.107982>.
- [12] J. Liu, R. Liu, P. Gray, Z. Liu, X. Cui, G. Li, Z. Liu, Development of a luciferase reporter Jurkat cell line under the control of endogenous interleukin-2 promoter, *J. Immunol. Methods* 451 (2017) 48–53, <https://doi.org/10.1016/j.jim.2017.08.006>.
- [13] J. Huang, L. Wang, C. Yu, Z. Fu, C. Liu, G. Wu, L. Guo, X. Guo, S. Chen, X. Liu, J. Wang, Development of a robust bioassay of monoclonal antibodies and biosimilars against TNF-alpha by NF-kappaB-inducible lentiviral reporter gene, *Int. Immunopharmacol.* 93 (2021), 107418, <https://doi.org/10.1016/j.intimp.2021.107418>.
- [14] M. Li, L. Wang, C. Yu, J. Wang, Development of a robust reporter gene assay for measuring the bioactivity of OX40-targeted therapeutic antibodies, *Luminescence* 36 (2021) 885–893, <https://doi.org/10.1002/bio.4004>.
- [15] Z. Fu, C. Yu, L. Wang, K. Gao, G. Xu, W. Wang, J. Cao, J. Wang, Development of a robust reporter gene based assay or the bioactivity determination of IL-5-targeted therapeutic antibodies, *J. Pharmaceut. Biomed* 148 (2018) 280–287, <https://doi.org/10.1016/j.jpba.2017.09.032>.
- [16] D.M. Jones, K.A. Read, K.J. Oestreich, Dynamic roles for IL-2-STAT5 signaling in effector and regulatory CD4(+) T cell populations, *J. Immunol.* 205 (2020) 1721–1730, <https://doi.org/10.4049/jimmunol.2000612>.
- [17] C. Haeuser, P. Goldbach, J. Huwyler, W. Friess, A. Allmendinger, Excipients for room temperature stable freeze-dried monoclonal antibody formulations, *J. Pharm. Sci. US* 109 (2020) 807–817, <https://doi.org/10.1016/j.xphs.2019.10.016>.
- [18] V.F. Arce, A. Furness, I. Solomon, K. Joshi, L. Mekkaoui, M.H. Lesko, R.E. Miranda, R. Dahan, A. Georgiou, A. Sledzinska, A.A. Ben, D. Franz, S.M. Werner, Y. Wong, J.Y. Henry, T. O'Brien, D. Nicol, B. Challacombe, S.A. Beers, S. Turajlic, M. Gore, J. Larkin, C. Swanton, K.A. Chester, M. Pule, J.V. Ravetch, T. Marafioti, K.S. Peggs, S.A. Quezada, Fc-optimized anti-CD25 depletes tumor-infiltrating regulatory T cells and synergizes with PD-1 blockade to eradicate established tumors, *Immunity* 46 (2017) 577–586, <https://doi.org/10.1016/j.immuni.2017.03.013>.
- [19] I. Kramer, J. Thiesen, A. Astier, Formulation and Administration of Biological Medicinal Products, *Pharm. Res.-Dordr.* 37 (2020) 159, <https://doi.org/10.1007/s11095-020-02859-z>.
- [20] International Conference on Harmonization Guidelines: ICH Q2(R1). Validation of Analytical Procedures: Text And methodology, 2005, pp. 6–13. http://www.ich.org/fileadmin/Public_Web_Site/ICH_Products/Guidelines/Quality/Q2_R1/Step4/Q2_R1_Guideline.
- [21] International Conference on Harmonization Guidelines: ICH Q6B. Specifications: Test Procedures and Acceptance Criteria for Biotechnological/biological Products, 1999, pp. 2–16. <https://database.ich.org/sites/default/files/Q6B%20Guideline.pdf>.
- [22] International Conference on Harmonization Guidelines, ICH Q14. Analytical Procedure Development, 2022, pp. 37–58. https://database.ich.org/sites/default/files/ICH_Q14_Document_Step2_Guideline_2022_0324.pdf.
- [23] F. Borriello, M. Longo, R. Spinelli, A. Pecoraro, F. Granata, R.I. Staiano, S. Loffredo, G. Spadaro, F. Beguinot, J. Schroeder, G. Marone, IL-3 synergizes with basophil-derived IL-4 and IL-13 to promote the alternative activation of human monocytes, *Eur. J. Immunol.* 45 (2015) 2042–2051, <https://doi.org/10.1002/eji.201445303>.
- [24] R. Moriggl, S. Berchtold, K. Friedrich, G.J. Standke, W. Kammer, M. Heim, M. Wissler, E. Stocklin, F. Gouilleux, B. Groner, Comparison of the transactivation domains of Stat5 and Stat6 in lymphoid cells and mammary epithelial cells, *Mol. Cell Biol.* 17 (1997) 3663–3678, <https://doi.org/10.1128/MCB.17.7.3663>.
- [25] D.E. Johnson, R.A. O'Keefe, J.R. Grandis, Targeting the IL-6/JAK/STAT3 signalling axis in cancer, *Nat. Rev. Clin. Oncol.* 15 (2018) 234–248, <https://doi.org/10.1038/nrclinonc.2018.8>.
- [26] S. Kang, T. Tanaka, M. Narazaki, T. Kishimoto, Targeting interleukin-6 signaling in clinic, *Immunity* 50 (2019) 1007–1023, <https://doi.org/10.1016/j.immuni.2019.03.013>.
- [27] A. Tobio, G. Bandara, D.A. Morris, D.K. Kim, M.P. O'Connell, H.D. Komarow, M.C. Carter, D. Smrz, D.D. Metcalfe, A. Olivera, Oncogenic D816V-KIT signaling in mast cells causes persistent IL-6 production, *Haematologica* 105 (2020) 124–135, <https://doi.org/10.3324/haematol.2018.212126>.
- [28] I. Karagiannidis, S.J. Jerman, D. Jacenik, B.B. Phinney, R. Yao, E.R. Prossnitz, E.J. Beswick, G-CSF and G-CSFR modulate CD4 and CD8 T cell responses to promote colon tumor growth and are potential therapeutic targets, *Front. Immunol.* 11 (2020) 1885, <https://doi.org/10.3389/fimmu.2020.01885>.
- [29] S. Biethahn, F. Alves, S. Wilde, W. Hiddemann, K. Spiekermann, Expression of granulocyte colony-stimulating factor and granulocyte-macrophage colony-stimulating factor-associated signal transduction proteins of the JAK/STAT pathway in normal granulopoiesis and in blast cells of acute myelogenous leukemia, *Exp. Hematol.* 27 (1999) 885–894, [https://doi.org/10.1016/s0301-472x\(99\)00017-x](https://doi.org/10.1016/s0301-472x(99)00017-x).
- [30] L. Cattaruzza, A. Gloghini, K. Olivo, R. Di Francia, D. Lorenzon, R. De Filippi, A. Carbone, A. Colombatti, A. Pinto, D. Aldinucci, Functional coexpression of Interleukin (IL)-7 and its receptor (IL-7R) on Hodgkin and Reed-Sternberg cells: involvement of IL-7 in tumor cell growth and microenvironmental interactions of Hodgkin's lymphoma, *Int. J. Cancer* 125 (2009) 1092–1101, <https://doi.org/10.1002/ijc.24389>.
- [31] S.L. Locatelli, A. Giacomini, A. Guidetti, L. Cleris, R. Mortarini, A. Anichini, A.M. Gianni, C. Carlo-Stella, Perifosine and sorafenib combination induces mitochondrial cell death and antitumor effects in NOD/SCID mice with Hodgkin lymphoma cell line xenografts, *Leukemia* 27 (2013) 1677–1687, <https://doi.org/10.1038/leu.2013.28>.
- [32] Y. Trieu, X.Y. Wen, B.F. Skinnider, M.R. Bray, Z. Li, J.O. Claudio, E. Masih-Khan, Y.X. Zhu, S. Trudel, J.A. McCart, T.W. Mak, A.K. Stewart, Soluble interleukin-13Ralpha2 decoy receptor inhibits Hodgkin's lymphoma growth in vitro and in vivo, *Cancer Res.* 64 (2004) 3271–3275, <https://doi.org/10.1158/0008-5472.ccr-03-3764>.
- [33] M. Binder, F.N. Vogtle, S. Michelfelder, F. Muller, G. Illerhaus, S. Sundararajan, R. Mertelsmann, M. Trepel, Identification of their epitope reveals the structural basis for the mechanism of action of the immunosuppressive antibodies basiliximab and daclizumab, *Cancer Res.* 67 (2007) 3518–3523, <https://doi.org/10.1158/0008-5472.CCR-06-3919>.
- [34] H. Ali, A. Mohiuddin, A. Sharma, I. Shaheen, J.J. Kim, K.M. El, A. Halawa, Implication of interleukin-2 receptor antibody induction therapy in standard risk renal transplant in the tacrolimus era: a meta-analysis, *Clin. Kidney J.* 12 (2019) 592–599, <https://doi.org/10.1093/ckj/sfy132>.
- [35] [a] International Conference on Harmonisation, Guidance on Q11 development and manufacture of drug substances; availability, *Not. Fed. Regist.* 77 (2012) 69634–69635; [b] S.L. Gaffen, K.D. Liu, Overview of interleukin-2 function, production and clinical applications, *Cytokine* 28 (2004) 109–69635, <https://doi.org/10.1016/j.cyt.2004.06.010>.
- [36] T. Burnouf, C.Y. Lee, C.W. Luo, Y.P. Kuo, M.L. Chou, Y.W. Wu, Y.H. Tseng, C.Y. Su, Human blood-derived fibrin releasates: composition and use for the culture of cell lines and human primary cells, *Biologicals* 40 (2012) 21–30, <https://doi.org/10.1016/j.biologicals.2011.09.017>.
- [37] P. Li, S. Mitra, R. Spolski, J. Oh, W. Liao, Z. Tang, F. Mo, X. Li, E.E. West, D. Gromer, J.X. Lin, C. Liu, Y. Ruan, W.J. Leonard, STAT5-mediated chromatin interactions in superenhancers activate IL-2 highly inducible genes: functional dissection of the Il2ra gene locus, *Proc. Natl. Acad. Sci. U.S.A.* 114 (2017) 12111–12119, <https://doi.org/10.1073/pnas.1714019114>.
- [38] Du JH, Yang D, Zhang J, Wang H, Guo B, Peng Y, Guo J, Ding, Structural basis for the blockage of IL-2 signaling by therapeutic antibody basiliximab, *J. Immunol.* 184 (2010) 1361–1368, <https://doi.org/10.4049/jimmunol.0903178>.
- [39] J. Damoiseaux, The IL-2 - IL-2 receptor pathway in health and disease: the role of the soluble IL-2 receptor, *Clin. Immunol.* 218 (2020), 108515, <https://doi.org/10.1016/j.clim.2020.108515>.